ISIJ International, Vol. 46 (2006), No. 11, pp. 1635–1644

Measurement and Prediction of Lubrication, Powder Consumption, and Oscillation Mark Profiles in Ultra-low Carbon Steel Slabs

Ho-Jung SHIN,[1] Seon-Hyo KIM,[1] Brian G. THOMAS,[4] Go-Gi LEE,[1] Je-Min PARK[2] and Joydeep SENGUPTA[3]

1) Department of Materials Science and Engineering, Pohang University of Science and Technology (POSTECH), Pohang, Kyoungbuk, 790-784, Republic of Korea. E-mail: seonhyo@postech.ac.kr 2) Steelmaking Department, POSCO Gwangyang Works, Gwangyang, Jeonnam, 545-711, Republic of Korea. 3) Research & Development, Dofasco Inc., Hamilton, Ontario Canada L8N 3J5. 4) Department of Mechanical and Industrial Engineering, University of Illinois at Urbana-Champaign, Urbana, IL 61081, USA.

(*Received on May 11, 2006; accepted on September 1, 2006*)

The flow of melted mold powder into the interfacial gap between the strand and the mold wall is important for productivity and quality in continuous cast slabs. Some of the mold slag (flux) consumption provides true lubrication, while much of the rest is trapped in the oscillation marks on the slab surface. This work presents measurements of powder consumption from extensive careful plant trials on ultra-low carbon steels, and a new, simple, semi-empirical model to predict slag consumption. The model predicts "lubrication consumption" by deducting the slag carried in the oscillation marks from the measured total. The oscillation mark shape is estimated from a theoretical analysis of equilibrium meniscus shape, which is based on metallographic analysis of many hook and oscillation mark shapes. The model demonstrates that the fraction consumed in the oscillation marks decreases with increasing casting speed, because the oscillation mark depth depends more on casting speed than on mold oscillation conditions. The model is validated by successful prediction of known trends of oscillation mark depth and mold powder consumption with changing various operation parameters. The model provides new insight into mold lubrication phenomena, which is important for extending casting operation to higher speeds and new lubrication regimes.

KEY WORDS: continuous casting; mold powder; slag; flux; lubrication; oscillation marks; mold oscillation; stroke; frequency; modification ratio; negative strip time; positive strip time; casting speed; meniscus; models; plant experiments.

1. Introduction

In the conventional continuous casting of steel, either mold powder or oil can be added to lubricate the mold from sticking to the solidifying steel shell. The mold powder melts to form a molten slag or flux layer, and also acts to protect the molten steel from oxidation, to insulate the molten steel from heat loss, to absorb inclusions from the molten steel, to regulate heat transfer to mold wall, and to minimize the formation of surface defects.[1,2] Thus, most of world's steel production is continuous-cast using slag lubrication,[3] which leads to more uniform and usually lower heat transfer between the strand and the mold wall compared with oil lubrication.[4] The slag infiltrates into the narrow gap between the surface of the shell and mold, and creates an "interfacial layer," as shown in **Fig. 1**(a), which controls both mold heat transfer and lubrication. A thicker interfacial layer is associated with a higher rate of flux infiltration into the gap. This provides better lubrication and lowers heat flux.[5] It also improves heat flux uniformity, which decreases surface defects.[6]

To maintain stable continuous casting, enough mold slag must infiltrate between the solidifying shell and the mold wall to lower friction, prevent sticking, and avoid defects and sticker breakouts. Ideally, the slag consumption should be large enough to maintain a continuous molten slag layer over the entire surface of the strand in the mold. The mold powder consumption decreases as the casting speed (v_s in mm s^{-1}) increases.[7–11] This restricts operation with higher casting speed, because breakouts are more likely to occur due to the thinner shell thickness[12] and higher frictional force[8] during high speed casting.

Consumption is readily measured by counting the mass of mold powder added per unit time (kg/s). Normalized consumption per unit area of strand (Q_{area} in kg m^{-2}) is a better way to represent lubrication, because it provides a measure of the mean flux thickness between the solidifying shell and the mold wall that is independent of mold perimeter, so long as consumption is uniform. Liquid layer thickness is sometimes estimated from the density of liquid slag (ρ_{slag} in kg m^{-3}), *i.e.* $d_{gap}=Q_{area}/\rho_{slag}$. However, this relation is inaccurate because it neglects the velocity gradients which exist across the liquid flux layer, the flux transported by the moving solid layer, and the flux consumed in the oscillation marks.[13]

The interfacial gap consists of layers of liquid and solid

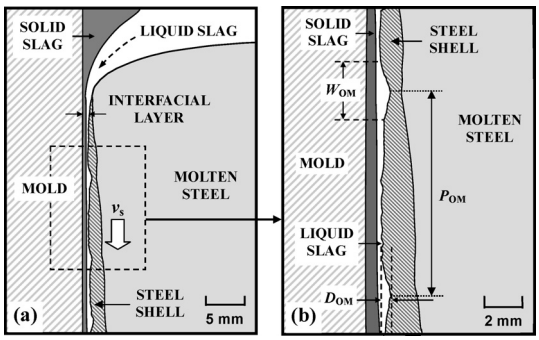

Fig. 1. Schematic diagram of interfacial gap between the mold and solidifying shell in continuous casting process.

slag as shown in Fig. 1(a). The solid slag layers are glassy, crystalline, or mixtures of both[14] depending on the slag composition and local cooling rate history.[15–17] Several previous models of heat transfer and lubrication assume that the gap has a uniform thickness.[18–20] However, the real strand surface contains periodic transverse depressions called oscillation marks (OM) in Fig. 1(b). The volume of these depressions generally consumes a significant amount of slag, which greatly affects lubrication and leads to non-uniform heat transfer in the mold.[21] Thus, quantifying the oscillation mark shape is a necessary prerequisite for the prediction of lubrication and heat transfer in the mold.

In this study, mold powder consumption was measured during casting trials conducted at POSCO Gwangyang Works for several different oscillation conditions and casting speeds. The measured consumptions were divided into two components: 1) the slag entrapped in the oscillation marks and 2) the remaining flux, which provides lubrication to prevent sticking, as shown in Fig. 1(b). This "lubrication consumption" is a more realistic concept to represent lubrication than total mold powder consumption.[17] The oscillation mark shape is calculated by combining measured OM depths with a realistic profile based on fundamentals.[22] Correlations are found for OM depth, corresponding OM consumption, lubrication, and powder consumption. Finally, the relations are applied to quantify the effect of various operating parameters, validating with measurements whenever possible.

2. Previous Work on Mold Powder Consumption

Many previous studies have attempted to relate powder consumption to the physical and chemical properties of the mold slag and the casting operation conditions. Wolf developed an empirical rule to select the optimal mold slag viscosity to minimize mold friction for a given casting speed,[23] and further to predict the optimal consumption rate[24] to provide stable operating conditions without breakouts. However, powder consumption also depends on other casting variables such as mold oscillation conditions,[1] and the temperatures related to crystallization of the mold flux.[1,25] Several other empirical equations have estimated the mold powder consumption as a function of various combinations of these parameters.[7,11,26–28]

2.1. Effect of Mold Powder Characteristics

The choice of mold powder greatly affects the consumption rate. Mills and Fox[1] report that mold flux performance varies with the mold dimensions, casting conditions and steel grade, as lubrication and horizontal heat transfer rate depend on the viscosity and break temperature of the liquid slag and the crystalline fraction of the slag rim. Decreasing liquid slag viscosity (taken at a standard temperature of 1 300°C) is well-known to increase consumption.[7,11,19,23,27,29,30] Tsutsumi *et al.*[11] have proposed that lower crystallization temperature increases powder consumption. The melting rate of the mold powder is also very important, because it must be fast enough to supply molten slag to match the consumption rate, while not being too high, so that liquid slag builds up and resolidifies as crust or excessive slag rims. The melting rate increases with lower free carbon contents, bulk density, and higher carbonate contents.[10]

2.2. Effect of Casting Speed

Casting speed is the most obvious parameter affecting powder consumption. Many regression equations based on powder consumption measurements in industry quantify that powder consumption decreases with higher casting speed.[7,23,27,31] Tsutsumi *et al.*[11] found that consumption ($kg\,m^{-2}$) varies inversely with casting speed if mold powder properties and oscillation conditions are kept constant. Some[32] claim that gravity is the main driving force for flux consumption, while others believe that consumption depends on interfacial frictional forces between the mold wall and shell, especially at high speed. Nakato *et al.*[33] found that the frictional force was a minimum value at a particular range of casting speeds (*e.g.* 1.2–1.4 m/min), which depends on mold powder properties. Moreover, liquid friction increases with higher casting speed.[8,34] Using a thermal-fluid-stress model of the interfacial gap, Meng and Thomas[17] found that friction depends critically on the lubrication consumption rate, and that the solid slag layer can fracture if this falls below a critical rate. Therefore, achieving adequate mold lubrication is essential for continuous casting at high speed.

2.3. Effect of Mold Oscillation Conditions

Mold oscillation with negative strip is essential for stable continuous casting,[35,36] and controls the frictional force between the solidifying shell and the mold wall. The industrial trend of increasing oscillation frequency to ~2–3 Hz helps to lower oscillation mark depth, with consequent surface quality improvement, especially in crack sensitive peritectic grades. However, the effect of individual mold oscillation parameters on lubrication are difficult to measure, because their effect is obscured by other important effects (*e.g.* casting speed), and they vary together with many other parameters, such as oscillation mark depth, and negative strip time, which are impossible to isolate. Break-outs can happen with shallower shell thickness or problems with sticking to the mold if the negative strip time is too short.

Non-sinusoidal oscillation provides an additional degree of flexibility in choosing oscillation conditions, relative to the traditional sinusoidal oscillator as shown in **Fig. 2**. This new mold oscillation method, sharpens the mold velocity change during downward motion in each oscillation cycle.[8,37,38] This mode has 3 independent mold oscillation parameters: oscillation stroke (s), frequency (f) and modification ratio (α). Modification ratio is defined as the time shift of the highest (or lowest) peak from the corresponding sinusoidal peak, compared to one quarter of the total period of the oscillation cycle. Other important parameters, such as negative strip time (t_n) and positive strip time (t_p) depend only on these 3 independent oscillation parameters and the casting speed, as defined elsewhere.[37–40] The negative strip time, or 'heal time',[3,16,41] is the time period when the mold is moving faster than the casting speed and the positive strip time is the rest of the oscillation cycle.

(i) Stroke Effect: Lengthening the stroke is reported to consume more powder per unit area.[7,11,27] Araki and

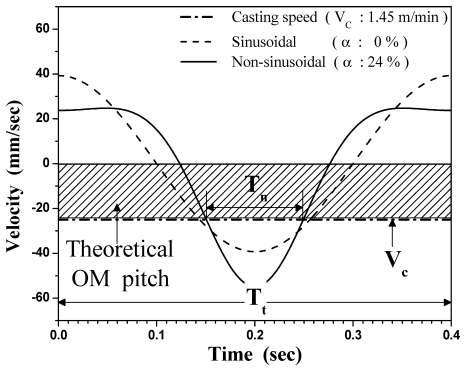

Fig. 2. Typical sinusoidal and non-sinusoidal oscillation modes studied.

Ikeda[28] interpret this observation with the concept of negative strip distance and propose that longer stroke and higher modification ratio should improve mold lubrication by increasing the negative strip distance. Kawamoto *et al.*[32] interpret alternatively that this effect is due to increased pressure during the oscillation downstroke.

(ii) Frequency Effect: The measured powder consumption per unit area of strand surface decreases greatly with increasing oscillation frequency.[27,42] This important influence of frequency on powder consumption was also found when stroke and casting speed were kept constant.[43]

(iii) Modification Ratio Effect: Higher modification ratio was reported to lower frictional force and to increase mold powder consumption.[8]

(iv) Negative Strip Time Effect: One of most popular indicators of powder consumption is negative strip time. During this time, the frictional force in the mold changes from tensile to compressive, so that any steel that is sticking to the mold wall will be squeezed onto the existing shell and 'stripped' from the mold wall. This important concept includes all 3 independent oscillation parameters in addition to the casting speed. The measured powder consumption per unit length measured in each oscillation cycle (q_{cycle}, $\text{g m}^{-1}\,\text{cycle}^{-1}$) increases in direct proportion with increasing negative strip time.[16,38,44] Computations of flow in the flux channel during oscillation suggest that this is due to the pressure from negative strip, although flux is predicted to be consumed during the positive strip time as well.

(v) Positive Strip Time Effect: Another powerful indicator of powder consumption is positive strip time. Powder consumption measured per unit area appears to increase with increasing positive strip time.[7,30] Powder consumption per unit length in a cycle of mold oscillation correlates very strongly with positive strip time.[8,9,11,28,34,38,45] Shin *et al.*[38] explained this stronger correlation because the positive strip time per cycle depends mainly on frequency at constant casting speed.

3. Experimental Trials

Plant measurements of mold powder consumption and oscillation mark depth were conducted on a conventional parallel-mold continuous slab caster at POSCO Gwangyang Works #2-1 Caster in 2002. The mold is equipped with a hydraulic mold oscillator, which allows a variety of non-sinusoidal oscillation modes in addition to changing stroke and frequency. The composition and properties of the ultra-low carbon steel grade cast and mold powder are given in **Table 1**. Experiments were performed in two groups: A), with varying oscillation conditions and similar casting speed (24.3–25.0 mm s^{-1}) and B), with different casting speeds (22.5–27.7 mm s^{-1}) and oscillation conditions changing with casting speed, as shown in **Table 2**. The trials in Group A were conducted with constant stroke, modification ratio, and frequency. Those of Group B were performed with constant modification ratio, frequency coefficient, *i.e.* $C_f = f/v_s$ and stroke coefficient, *i.e.* $C_s = s/v_s$. The casting conditions and results of Trials A and B are presented in Table 2, for 21 sequences where conditions were maintained virtually constant and used the same mold powder (Table 1).

The mold powder consumption per unit strand area, Q_{area}, was calculated from the weight of the bags consumed during each entire sequence, Q_{cons}, which includes over 20 000 oscillation marks (200–300 m of cast length).

$$Q_{\text{area}} = \frac{Q_{\text{cons}}}{V_C \times (2W + 2N)} \quad \text{.....(1)}$$

Table 1. Composition and properties of steel and mold powder.

I. Steel:	
C (0.002~0.005%) – **Mn** (0.07~0.15%) – **Si** (≤ 0.005%) – **P** (0.01%) – **S** (0.01~0.012%) – **Cr** (0.01%) – **Ni** (≤0.01%) – **Cu** (≤0.01%) – **Ti** (0.025~0.05%) – **Al_{tot}** (0.035%)	
Density of liquid steel (kg m^{-3})	7127
Surface tension at 1550 °C (N m^{-1})	1.6
Liquidus temperature (°C)	1534
Solidus temperature (°C)	1519
*II. Mold Powder (**Trial A** and **B**):*	
CaO (39.8%) – **SiO_2** (36.3%) – **Al_2O_3** (3.4%) – **MgO** (0.8%) – **Li_2O** (0.4%) – **Na_2O** (3.4%) – **K_2O** (0.1%) – **Fe_2O_3** (0.3%) – **MnO_2** (0.03%) – **TiO_2** (0.2%) – **F** (6.0%) – **CO_2** (3.5%) – **C_{total}** (3.0%)	
Density of liquid slag (kg m^{-3})	2680
Viscosity at 1300 °C (Pa s)	0.321
Surface tension (N m^{-1})	0.431
Solidification temperature (°C)	1145
Melting temperature (°C)	1180
*III. Mold Powder (**Trial C**):*	
CaO (37.9%) – **SiO_2** (37.8%) – **Al_2O_3** (5.0%) – **MgO** (2.0%) – **Li_2O** (0.9%) – **Na_2O** (3.8%) – **K_2O** (0.1%) – **Fe_2O_3** (0.3%) – **MnO_2** (0.04%) – **TiO_2** (0.3%) – **F** (7.2%) – **CO_2** (3.2%) – **C_{total}** (2.6%)	
Density of liquid slag (kg m^{-3})	2660
Viscosity at 1300 °C (Pa s)	0.262
Surface tension (N m^{-1})	0.419
Solidification temperature (°C)	1101
Melting temperature (°C)	1145

Table 2. Operation conditions and measurement of powder consumption from plant trials.

Test No.	Casting width (mm)	Casting speed (mm/s)	oscillation Stroke (mm)	oscillation frequency (Hz)	Modification ratio (%)	Negative strip time (s)	Positive strip time (s)	Mold powder consumption (kg/m^2)
A-1	1300	24.4	6.44	2.65	24	0.107	0.270	0.247
A-2	1300	24.3	5.00	2.43	0	0.115	0.296	0.232
A-3	1300	24.5	5.00	2.94	12	0.100	0.241	0.225
A-4	1300	24.9	5.00	3.49	24	0.081	0.205	0.253
A-5	1300	25.0	6.00	2.08	12	0.127	0.353	0.223
A-6	1300	24.5	6.00	2.45	24	0.110	0.299	0.229
A-7	1300	24.8	6.00	2.90	0	0.121	0.224	0.230
A-8	1300	24.8	7.00	1.77	24	0.139	0.426	0.248
A-9	1300	24.4	7.00	2.09	0	0.154	0.324	0.208
A-10	1300	24.9	7.00	2.49	12	0.126	0.276	0.211
B-1	1570	22.5	6.25	2.46	24	0.114	0.292	0.271
B-2	1570	23.0	6.30	2.52	24	0.112	0.285	0.247
B-3	1570	23.7	6.37	2.58	24	0.109	0.278	0.256
B-4	1300	24.7	6.47	2.69	24	0.106	0.267	0.238
B-5	1300	24.6	6.46	2.67	24	0.106	0.268	0.237
B-6	1300	25.3	6.53	2.74	24	0.104	0.261	0.215
B-7	1300	25.8	6.58	2.79	24	0.102	0.256	0.212
B-8	1050	27.5	6.75	2.96	24	0.097	0.241	0.210
B-9	1050	27.7	6.77	2.97	24	0.097	0.240	0.194
B-10	1300	24.4	6.44	2.66	24	0.107	0.270	0.247
B-11	1300	25.0	6.50	2.71	24	0.105	0.264	0.234

A second trial was conducted to measure oscillation mark depth. The narrow faces of each 100 mm long slab sample cast were sectioned and sand-blasted to remove any scale on the surface. The oscillation mark shape and depth were measured with a profilometer across slab thickness (230 mm) in steps of 10 mm. The results are presented in **Table 3**. The oscillation marks here are much smaller than those observed by Itoh *et al.*[46]

3.1. Total Mold Powder Consumption

The measured powder consumption per unit area can be converted to total consumption per unit length in a cycle of mold oscillation, q_{cycle}, by multiplying by the theoretical pitch of the oscillation marks $(P_{\text{OM}})_{\text{theoretical}} = v_s/f$,

Table 3. Operation conditions and measured depth of oscillation marks from plant trials.

Test No.	Casting width (mm)	Casting speed (mm/s)	Solidification temperature of mold powder (°C)	Viscosity of mold powder at 1300 °C (Pa·s)	Negative strip time (s)	Measured oscillation mark depth (mm)
A-1	1300	24.4	1149	0.321	0.107	0.246
A-2	1300	24.3	1149	0.321	0.115	0.393
A-3	1300	24.5	1149	0.321	0.100	0.309
A-4	1300	24.9	1149	0.321	0.081	0.292
A-5	1300	25.0	1149	0.321	0.127	0.353
A-6	1300	24.5	1149	0.321	0.110	0.343
A-7	1300	24.8	1149	0.321	0.121	0.258
A-8	1300	24.8	1149	0.321	0.139	0.308
A-9	1300	24.4	1149	0.321	0.154	0.338
A-10	1300	24.9	1149	0.321	0.126	0.331
C-1	1300	29.1	1101	0.262	0.100	0.251
C-2	1300	23.6	1101	0.262	0.118	0.328
C-3	1300	20.2	1101	0.262	0.134	0.280
C-4	1570	24.6	1101	0.262	0.115	0.313
C-5	1570	24.3	1101	0.262	0.116	0.272
C-6	950	30.0	1101	0.262	0.092	0.225
C-7	950	30.1	1101	0.262	0.092	0.214
C-8	950	29.9	1101	0.262	0.092	0.199
C-9	1300	28.2	1101	0.262	0.097	0.192
C-10	1300	23.3	1101	0.262	0.114	0.302
C-11	1300	28.1	1101	0.262	0.097	0.236
C-12	1300	28.1	1101	0.262	0.097	0.277
C-13	1570	22.9	1101	0.262	0.115	0.310
C-14	1570	22.9	1101	0.262	0.115	0.304
C-15	1570	16.5	1101	0.262	0.152	0.495
C-16	1570	13.9	1101	0.262	0.175	0.566

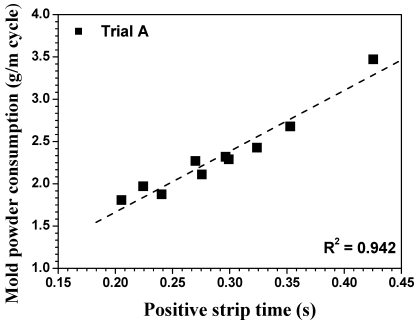

Fig. 3. Effect of positive strip time on mold powder consumption in each oscillation cycle.

$$q_{\text{cycle}} = Q_{\text{area}} \times (P_{\text{OM}})_{\text{theoretical}} = Q_{\text{area}} \times \frac{v_s}{f} \quad \text{.....(2)}$$

A regression was performed on the data collected for trial A to correlate q_{cycle} with positive strip time. As shown in **Fig. 3**, the relationship is nearly linear,

$$q_{\text{cycle}} = 7.195 \times t_p + 0.2256 \quad \text{.....(3)}$$

This correlation is similar to those of many other researchers[8,9,11,28,34,38,45] discussed in the previous section. To test its validity, this relationship with positive strip was compared with the powder consumption measurements of trial B, which were obtained for different casting speeds, with stroke and frequency increased in proportion with speed. Positive strip time thus decreased with increasing speed as well. Modification ratio was kept constant. The prediction of Eq. (3), (solid line) is compared with the measured data points in **Fig. 4**. Powder consumption clearly decreases with increasing casting speed but the measured and predicted lines do not quite match. Thus, powder consumption also depends on other parameters, such as oscillation mark depth.

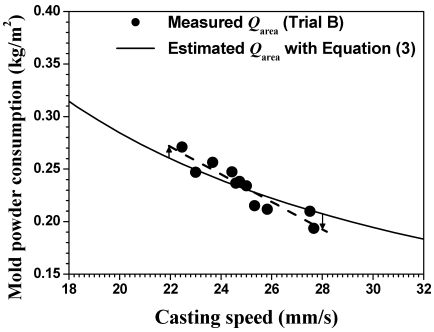

Fig. 4. Validation of powder consumption model with measurements at different casting speeds.

3.2. Oscillation Mark Depth

Oscillation mark depth was not measured during trial group B, so a third group of trials, Group C, was conducted. Casting conditions were kept similar, except for the mold powder composition, as shown in Table 1. The results are presented in Table 3, including the mean depth of the oscillation marks. Oscillation mark depth was correlated in this work with negative strip time and casting speed, as shown in Eq. (4). The stroke and frequency of mold oscillation were neglected because negative strip time roughly includes these effects, as t_n decreases with both decreasing stroke and increasing frequency.[38,40]

$$(D_{\text{OM}})_{\text{estimated}} = k \times t_n^{\,0.272} \times v_s^{\,-1.04} \quad \text{.....(4)}$$

where empirical constant k depends on powder properties; k_A (for Trials A and B) is 15.8 and k_C (for Trial C) is 14.0.

There are two possible reasons why k_C is lower than k_A. Firstly, the mold powder used for Group C has a lower solidification temperature and viscosity at 1 300°C than those for Group A and B, as given in Table 3. Bommaraju *et al.*[47] reported that mold powder with a lower solidification temperature, has shallower oscillation mark depth. This might be due to smaller slag rims.

The second reason is that the lower viscosity of the slag in Group C may allow easier steel overflow of the meniscus after it freezes during hook formation. This agrees with the modeling trends of Hill *et al.*[48] but not with that of Kobayashi and Maruhashi.[49] Further work is needed to include the effects of mold powder on oscillation mark depth beyond the simple constants (k) assumed here.

Figure 5(a) shows a reasonable fit between the measured oscillation mark depth and the correlation in Eq. (4). Shallower oscillation marks have been measured for faster casting speed[7,40] and shorter negative strip time,[8,30,40,44] which agrees with the results of this study, shown in Figs. 5(b) and 5(c). **Figure 6** shows the predicted effect of mold oscillation stroke and frequency on oscillation mark depth from Fig. 4. The slight increase in oscillation mark depth with increasing stroke and decreasing frequency agrees with previous results[7,39,40] as shown in Figs. 6(a) and 6(b). More important is the effect of increasing casting speed, which greatly lowers oscillation mark depth. This effect of casting speed dominates over the effect of oscillation conditions.

In most plant practices, the mold oscillation conditions change systematically with casting speed. Typically, oscillation frequency increases with casting speed to maintain constant negative strip time ratio, *i.e.* $NSTR = t_n/(t_n + t_p)$. In this case, the negative strip time decreases with increasing casting speed. The effect of *NSTR* on oscillation mark depth is plotted in Fig. 6(c), and is similar to that with negative strip time.[8,27,30,39,40,44] These results suggest that the

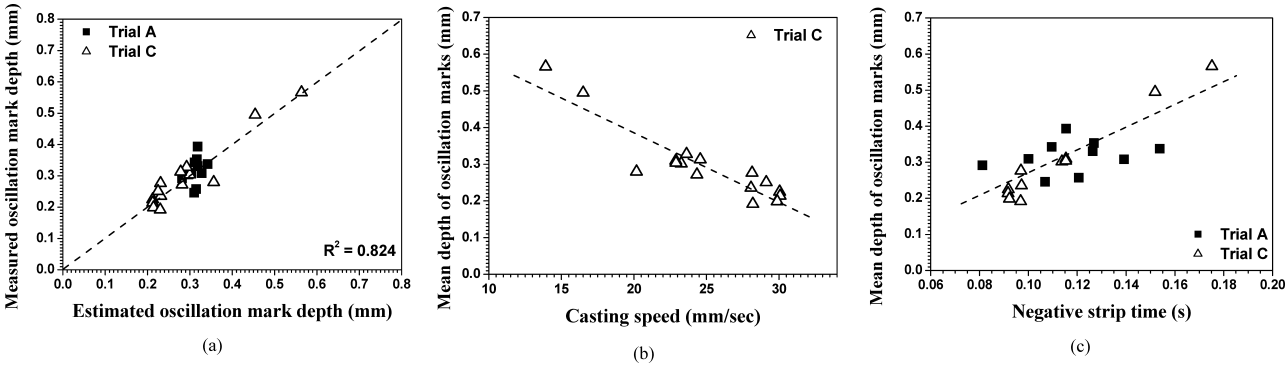

Fig. 5. (a) Comparison of the measured and estimated oscillation mark depth and effects of (b) casting speed and (c) local frequency on oscillation mark depth.

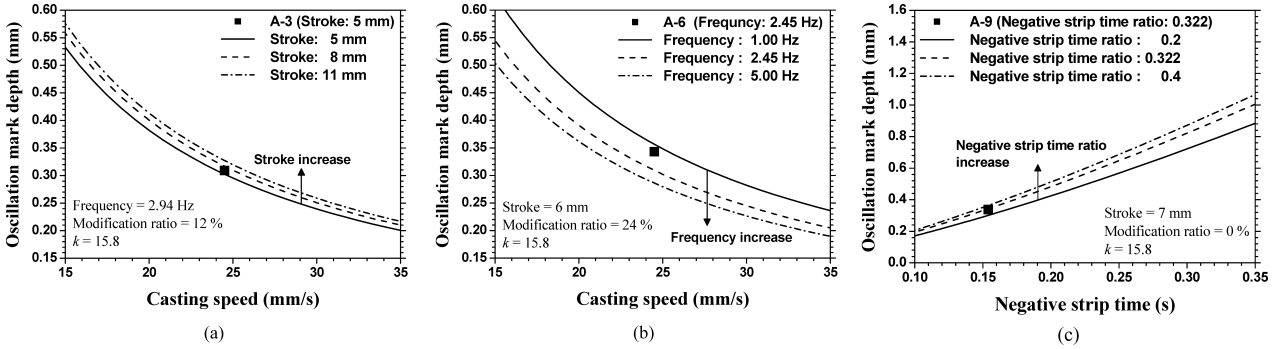

Fig. 6. Influence of mold oscillation (a) stroke, (b) frequency and (c) negative strip time ratio on oscillation mark depth.

apparent effect of oscillation conditions on oscillation mark depth may be an artifact of the cross-correlation with the more important effect of casting speed.

In this work, the trials of Group A were aimed at checking the effect of mold oscillation with the exclusion of casting speed effect. For this unique trial, the trends observed between oscillation mark depth and oscillation parameters (negative strip time in Eq. (4) and frequency in Fig. 5(c)) were relatively weak. Thus, other parameters which depend on casting speed, such as oscillation mark depth, should be incorporated more carefully as well, in predicting mold flux consumption.

4. New Model of Mold Powder Consumption

From Meng and Thomas,[17] mold powder consumption (Q_{area}) can be divided into three components in Eq. (5), shown in Fig. 1.

$$Q_{\text{area}} = Q_{\text{solid}} + Q_{\text{liquid}} + Q_{\text{OM}} \quad \text{.....(5)}$$

Firstly, Q_{solid} is the thick solid layer that resolidifies from the liquid slag onto the mold walls, and can move intermittently downward if it detaches from the mold wall.[13] Secondly, Q_{liquid} is the thin layer of continuous liquid slag that moves down at a speed between the casting speed and the solid layer speed.[17] Thirdly, Q_{OM} is the slag within the oscillation marks, which is carried down at the casting speed, and accounts for the majority of flux consumption at lower speed, when the oscillation marks are large. A fourth possible component is the extra slag consumption which may flow downward in regions of significant localized gap formation, where the shell pulls away from the mold, such as in the corner regions.

Both the liquid and solid slag layers help to prevent sticking, so in this model, Q_{liquid} and any non-zero Q_{solid} are considered together as "lubrication consumption". Local non-uniformities, such as corner effects, are ignored. Consumption per unit area of the strand surface, Q_{area}, (kg m^{-2}) is divided into two components: 'Oscillation mark consumption' (Q_{OM}) and 'Lubrication consumption' (Q_{lub}).

$$Q_{\text{area}} = Q_{\text{OM}} + Q_{\text{lub}} \quad \text{.....(6)}$$

Previous work by Thomas *et al.*[21] demonstrated that oscillation marks are generally filled with mold flux, so the component of slag consumption carried by the oscillation mark volume is defined as follows:

$$Q_{\text{OM}} = \rho_{\text{slag}} \times A_{\text{OM}} \times \frac{f}{v_s} \times \frac{1}{1\,000} \quad \text{.....(7)}$$

The total volume depends on the area of each oscillation mark, A_{OM}, given by its depth and width, and varies inversely with the pitch between marks. These geometric parameters are defined in Fig. 1(b). Thus, oscillation mark volume was determined as part of this work, based on the measurements of oscillation mark depth, described previously, and their assumed shape, described next.

4.1. Oscillation Mark Shape with Bikerman Equation

The oscillation mark shape corresponds with the equilibrium shape of the meniscus interface between the liquid steel and liquid slag.[46,50,51] Although the meniscus shape is known to vary during mold oscillation,[9,16,20,52] this phenomenon was ignored, due to its complexity and relatively minor effect on powder consumption. In this work, each oscillation mark is assumed to adopt the equilibrium shape of the frozen meniscus, featuring distinct bottom and top portions, which freeze before and after overflow respectively.

In the absence of any surface waves or dynamic motion, the equilibrium meniscus shape is determined by the balance of surface tension and gravity forces given by Bikerman's equation[22] below:

$$x - x_0 = -\sqrt{2a^2 - z^2} + \frac{a}{\sqrt{2}} \ln \frac{a\sqrt{2} + \sqrt{2a^2 - z^2}}{z} \quad \text{...(8)}$$

$$x_0 = a - \frac{a}{\sqrt{2}} \ln(\sqrt{2}+1) \quad \text{.....(9)}$$

$$a = \sqrt{\frac{2 \cdot \Delta\gamma}{\Delta\rho \cdot g}} \quad \text{.....(10)}$$

where, x is the distance perpendicular to the mold wall in m, z is the distance along the mold wall in m, $\Delta\gamma$ is the difference of surface tension between liquid steel and liquid slag in $\mathrm{N\,m^{-1}}$, $\Delta\rho$ is the dissimilarity of density between liquid steel and liquid slag in $\mathrm{kg\,m^{-3}}$, and g is the gravitational acceleration ($9.81\,\mathrm{m\,s^{-2}}$). The meniscus shape calculated by Eqs. (8)–(10) for the parameters in Table 1, is presented in **Fig. 7**. The surface tension between the liquid steel and vapor depends strongly on sulfur content in the steel.[53] A surface tension of $1.6\,\mathrm{N\,m^{-1}}$ is selected for ultra-low carbon steel corresponding to a sulfur content of 0.01%.[54,55] The steel density is assumed to be $7\,127\,\mathrm{kg\,m^{-3}}$.[56]

The sequence of events leading to the formation of subsurface hooks and the shape of oscillation marks is shown schematically in **Fig. 8**.[57] The steady meniscus shape is shown in Fig. 8(a). The meniscus may freeze suddenly to extend the solidifying shell tip, owing to the susceptibility to undercooling of ultra-low carbon steels relative to other grades.[58] The meniscus of heavy liquid steel supported above the freezing shell tip is precariously balanced by surface tension, as shown in Fig. 8(b). This quasi-stable situation quickly becomes unstable with the downward moving of shell, and the liquid steel starts to collapse under gravity. After the liquid steel has overflowed, the interfacial shape of the captured liquid slag and overflowing liquid steel should match the lower part of the Bikerman shape (Fig. 7) as shown in Fig. 8(c).

The shape of the frozen meniscus described by the upper part of the Bikerman equation in Fig. 7 should approximate the lower part of the oscillation mark. The lower part of the Bikerman equation should estimate the upper part. To evaluate the accuracy of this idea, the Bikerman shape in Fig. 7 is compared in **Fig. 9** with the measured shape of oscillation marks and hooks that were obtained on ~100 mm long steel slab sample produced under the condition of A-1 in Table 2. Figure 9(a) shows a typical curved hook adjacent to an oscillation mark etched with proper etching method[38,60] in one of the samples of Group A. The upper part of the Bikerman shape in Fig. 7 is compared with the lines measured from the slab surface along the lower part of the oscillation mark to end of hook as shown in Fig. 9(b). Although there is a variation of shapes, most of those are close to the upper part of Bikerman's shape. The lower part of the Bikerman shape is compared with the lines from the deepest part of the oscillation mark to its upper end, as shown in Fig. 9(c).

A typical example of a measured oscillation surface profile (A-1) is compared with the estimated shape based on the Bikerman equations as shown in Fig. 9(d). The estimated area slightly under predicts the measured area, especially considering that other surface depressions unrelated to oscillation marks are not considered. This approach using Bikerman equations gives estimated widths of oscillation marks of 1.2–2.2 mm, which are similar to the measured surface profiles of oscillation marks on the narrow face of ultra low carbon steel slabs by Bommaraju *et al.*[47] The area of the oscillation marks based on these Bikerman equations was used in developing correlations to predict flux consumption by oscillation marks.

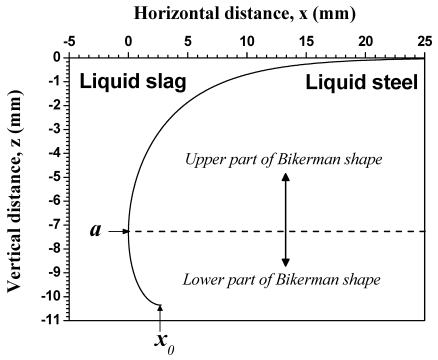

Fig. 7. Meniscus shape from Bikerman equation (Table 1 conditions).

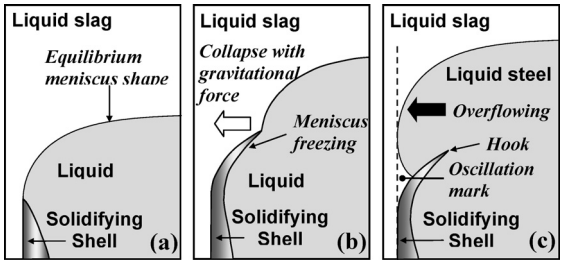

Fig. 8. Mechanism of oscillation mark shape and hook formation in ultra-low carbon steel slabs by (a) steady state, (b) meniscus freezing, and (c) subsequent liquid steel overflowing of meniscus.

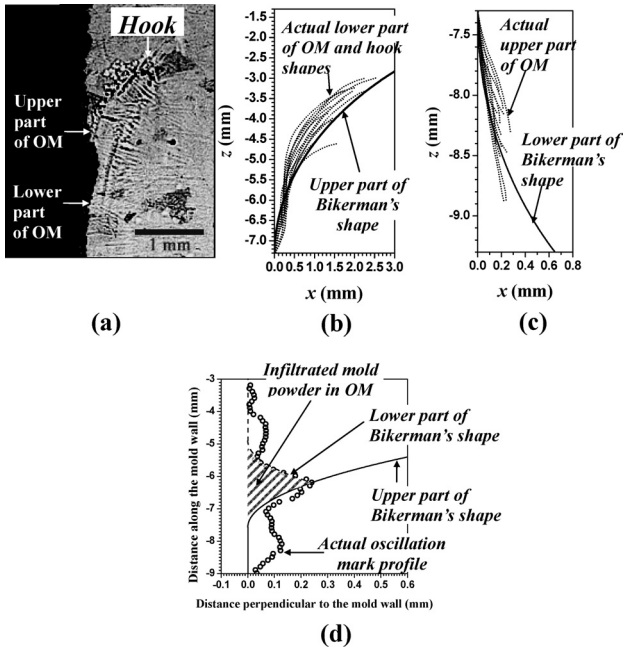

Fig. 9. (a) Typical oscillation mark and hook in an ultra-low carbon steel slab, (b) comparison of the measured shape of the lower part of oscillation marks and hooks with the upper part of Bikerman's equation, (c) comparison between measured shape of upper part of oscillation mark with the lower part of Bikerman's equation, and (d) comparison between actual oscillation mark profile and shape based on Bikerman's equation.

4.2. Estimation of Lubrication Consumption with Oscillation Mark Consumption

To estimate the powder consumption carried down in the oscillation marks, the area of each oscillation mark was calculated using Eqs. (11) and (12) and the measured depth of

the oscillation marks of Group A, given in Table 3.

$$(A_{OM})_{estimated} = \int_{z_1}^{z_2} \left(-\sqrt{2a^2 - z^2} + \frac{a}{\sqrt{2}} \ln \frac{a\sqrt{2} + \sqrt{2a^2 - z^2}}{z} + x_0 \right) dz \quad \text{.....(11)}$$

where, z_1, z_2 are the solutions of Eq. (12).

$$D_{OM} = -\sqrt{2a^2 - z^2} + \frac{a}{\sqrt{2}} \ln \frac{a\sqrt{2} + \sqrt{2a^2 - z^2}}{z} + x_0 \quad \text{.....(12)}$$

The estimated A_{OM} thus depends on parameters, a, Eq. (10), and D_{OM} (Eq. (12)), as shown in **Fig. 10**. A simpler empirical equation to estimate A_{OM} was then defined as follows:

$$(A_{OM})_{estimated} = 25 \times \left(\sqrt{\frac{2 \cdot \Delta\gamma}{\Delta\rho \cdot g}} \right)^{0.556} \times (D_{OM})^{1.43} \quad \text{...(13)}$$

Figure 11 compares the areas of actual oscillation mark profiles (measured with a profilometer) with estimates using Eq. (13), based on measured D_{OM}. The deviations in Fig. 11 indicate variations in oscillation mark shape from the idealized equilibrium shape assumed here, caused by unexpected events such as mold level fluctuation.

The flux consumed in the oscillation marks per cycle (q_{OM} in $g\,m^{-1}\,cycle^{-1}$) is then calculated from A_{OM} using Eqs. (2) and (7) as shown in Eq. (14).

$$q_{OM} = \rho_{slag} \times A_{OM} \times \frac{1}{1\,000} \quad \text{.....(14)}$$

Inserting Eq. (13) into Eq. (14), and estimating D_{OM} using Eq. (4), an approximate expression for oscillation mark consumption per cycle (q_{OM}) is derived as Eq. (15).

$$q_{OM} = 2.5 \times 10^{-2} \times \rho_{slag} \times k^{1.43} \times \left(\sqrt{\frac{2 \cdot \Delta\gamma}{\Delta\rho \cdot g}} \right)^{0.556} \times t_n^{0.389} \times v_s^{-1.49} \quad \text{.....(15)}$$

Figure 12(a) shows that the total mold powder consumption per cycle (q_{cycle}) from Eq. (3). Figure 3 is divided into oscillation mark consumption per cycle, q_{OM} and lubrication consumption per cycle, q_{lub} according to Eq. (6). Figure 12(b) shows the relative fractions of these two components of flux consumption, which are both significant.

Tsutsumi *et al.*[61] reported that the inflow ratio of mold powder during the positive strip time was 60% of the total powder consumption, based on observations of the periodic change of the distance between the mold wall and the solidifying shell in experiments on a Sn–Pb alloy (metal) and stearic acid (flux) system. Their direct observation of the formation of oscillation marks and mold flux consumption near the meniscus concluded that most oscillation marks formed due to meniscus overflow during the negative strip time. Badri *et al.*[62,63] observed rising mold heat flux during the negative strip time in their mold simulator. These results with two different mold simulators support that the meniscus freezes and overflows (Figs. 8(b) and 8(c)) during nega-

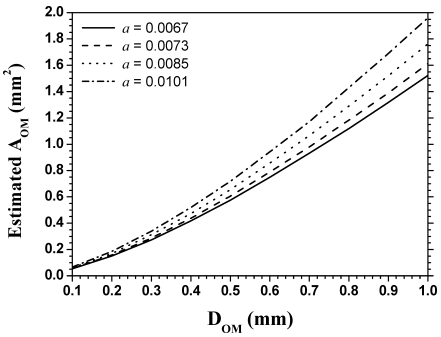

Fig. 10. Influence of oscillation mark depth on estimated area of oscillation mark with different distance from flat liquid surface to contact point of liquid and the mold wall calculated from Bikerman equations.

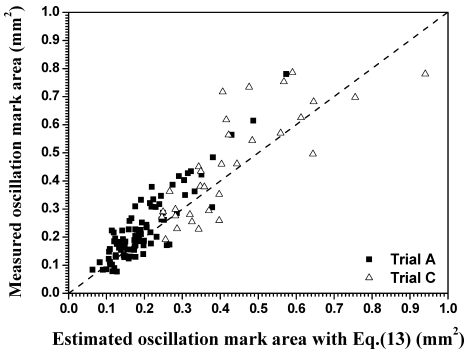

Fig. 11. Comparison of the measured and estimated oscillation mark area.

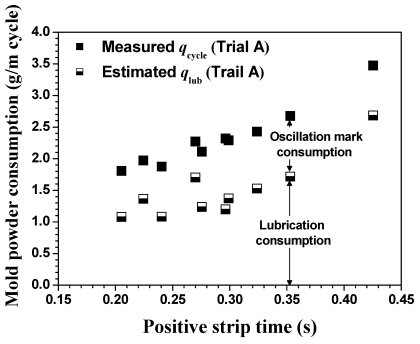

(a)

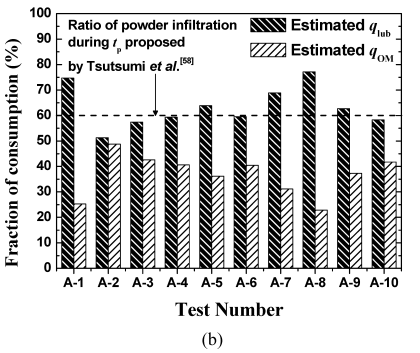

(b)

Fig. 12. Comparison of (a) consumption and (b) fraction of powder consumed in oscillation marks (OM) and providing lubrication (lub) during a mold oscillation cycle (Trial A).

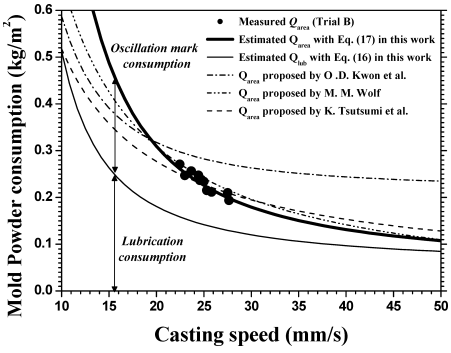

Fig. 13. Validation of predicted powder consumption per unit area with measurements taken at different casting speeds (Trial B) compared with other people's works.

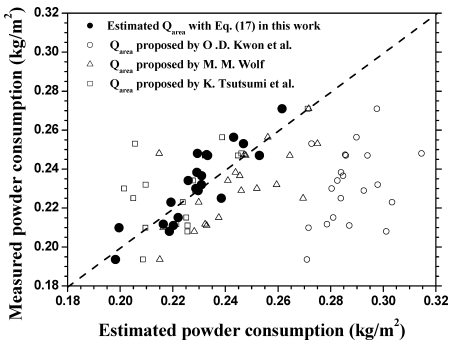

Fig. 14. Comparison of estimated powder consumption per unit strand area with measured powder consumption for Trial A and B in Table 2.

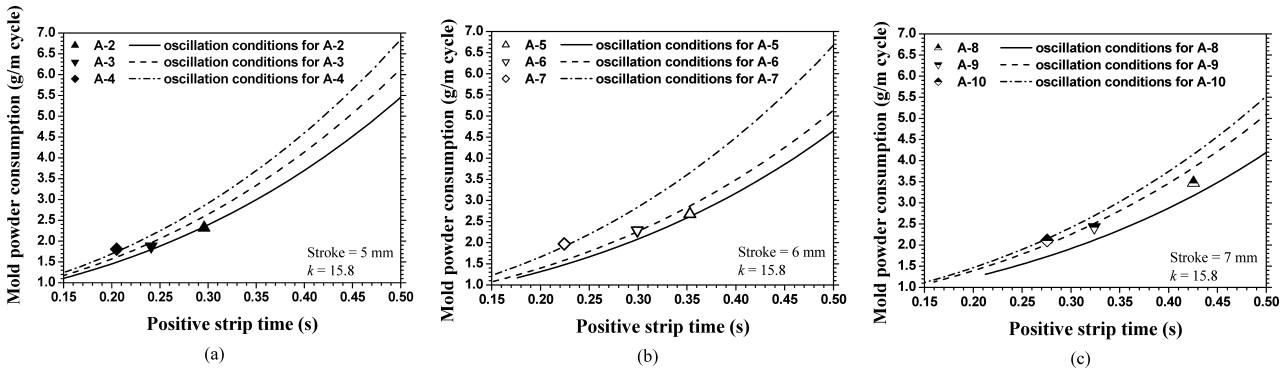

Fig. 15. Validation of predicted powder consumption per cycle with measurements of Group A taken at different strokes (a) 5 mm, (b) 6 mm, and (c) 7 mm.

tive strip time.[57,64] This further suggests that perhaps the oscillation mark consumption depends mainly on negative strip time and lubrication consumption occurs during positive strip time. Approximate expressions for consumption per cycle (q_{lub}) were derived based on the above idea, and incorporating the terms and main trends in Eqs. (1)–(15):

$$q_{\mathrm{lub}} = 0.507 \times e^{3.59 \times t_{\mathrm{p}}} \quad \text{.....(16)}$$

The total powder consumption per unit area (Q_{area}) is estimated with Eq. (2) and the sum of Eqs. (15) and (16).

$$Q_{\mathrm{area}} = (q_{\mathrm{OM}} + q_{\mathrm{lub}}) \times \frac{f}{v_{\mathrm{s}}} = \left(2.5 \times 10^{-2} \times \rho_{\mathrm{slag}} \times k^{1.43} \times \left(\sqrt{\frac{2 \cdot \Delta\gamma}{\Delta\rho \cdot g}} \right)^{0.556} \times t_{\mathrm{n}}^{0.389} \times v_{\mathrm{s}}^{-1.49} + 0.507 \times e^{3.59 \times t_{\mathrm{p}}} \right) \times \frac{f}{v_{\mathrm{s}}} \quad \text{.....(17)}$$

5. Discussion

These relations provide a clue to interpret initial solidification behavior and oscillation mark formation near meniscus in ultra low carbon steel. Previously, there have been two different groups of opinions about the formation of oscillation marks. One is a "bending theory," in which the tip of the solidifying shell bends under the positive pressure created in the flux channel from the downward movement of the mold during negative strip time.[29,52,65] The other is a "meniscus freezing theory," which has been already mentioned in Figs. 8. After freezing the meniscus and growing a solidifying shell tip, the shell tip will move down in less time if the casting speed is faster in Fig. 8(c). Thus, overflowing of the liquid steel is easier, leading to shallower oscillation marks even with the same negative strip time. The greater importance of casting speed in Eqs. (4) and (13) suggests that meniscus freezing and overflow is the dominant mechanism controlling initial solidification in ultra-low carbon steel.

6. Model Validation

The predicted powder consumption per unit area calculated with Eq. (17) is compared with measured consumption rates (Trial B) and with other literature correlations[7,11,23] as shown in **Fig. 13**. Having developed a more fundamental model for flux consumption, Eqs. (15) and (16), than the simple empirical relation, Eq. (3), Fig. 3 can be redrawn, distinguishing the effects of individual oscillation parameters. **Figure 14** shows that the new model to estimate powder consumption matches the measured powder consumption for Trial A and B given in Table 2 better than other correlations. The effect of positive strip time on flux consumption is shown in **Figs. 15**(a)–15(c), keeping the stroke constant in each frame. Each test of Group A has a different line in Fig. 11, matches with only one measured value, because each set of oscillation conditions for these tests was different in some way. As further validation, the predictions of the new model, Eqs. (15) and (16) are compared with powder consumption measurements for the data of Group B, in which both oscillation conditions and casting speed were varied, as previously discussed. **Figure 16** shows good agreement with the effect of positive strip time (g/m-cycle) and Fig. 13 shows good agreement with the effect of casting speed (kg/m^2). The agreement is clearly superior to that of Eq. (3) in Fig. 4.

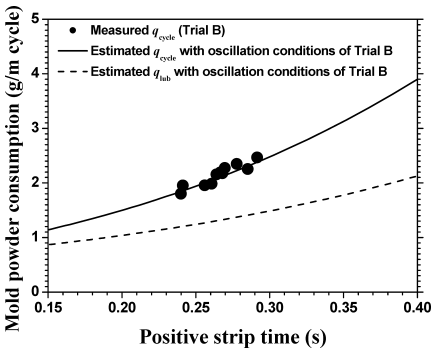

Fig. 16. Validation of predicted powder consumption with measurements (Trial B).

The linear correlation between powder consumption and positive strip time in Eq. (3) and Fig. 3 is thus concluded to be a coincidental result of the choice of test conditions. The correlation of total mold powder consumption per cycle with positive strip time is not a fundamental relation, because only lubrication consumption depends on positive strip time, Eq. (16). The difference between the solid and dotted lines in Figs. 16 and 13 is the estimated consumption by the oscillation marks during the negative strip time. Similar trends with positive and negative strip time are observed because both decrease with the increase in casting speed, and the increase in oscillation frequency with increasing casting speed.

The predicted lubrication consumption is presented in Figs. 16 and 13. The total powder consumption is well-known to decrease with casting speed up to 8 m/min.[32] The fraction of lubrication consumption increases with increasing casting speed, which agrees with the findings of Meng and Thomas.[17] This is due in part to the drop in oscillation

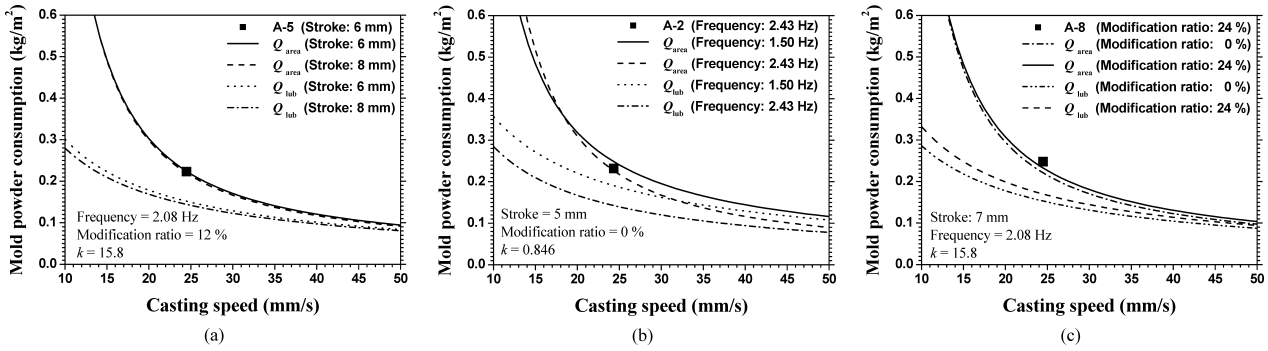

Fig. 17. Influence of (a) stroke, (b) frequency, and (c) modification ratio of mold oscillation on mold powder consumption per unit strand area.

mark depth with increasing casting speed.

7. Results

The new consumption model is easily applied to quantify the effect of individual mold oscillation conditions on lubrication. **Figure 17** plots the estimated total and lubrication consumption rates per unit area (Q_{area} and Q_{lub}) for different mold oscillation conditions, which are fixed while casting speed varies. In each figure, measured points are included as available, and all show a good match.

Oscillation stroke has almost no effect on powder consumption, as shown in Fig. 17(a). Increasing stroke is predicted to decrease powder consumption very slightly, which is contrary to the trends of other researchers.[7,11,27] This disagreement may arise because oscillation stroke affects the solid slag layer velocity, and needs more study.

Figure 17(b) shows the effect of oscillation frequency on mold powder consumption. Increasing frequency lowers the total consumption rate, which agrees with previous findings.[8,43] For the oscillation frequency of 2.43 Hz in Fig. 17(b), the difference between Q_{area} and Q_{lub} drops from $0.0854\,kg\,m^{-2}$ at $24.2\,mm\,s^{-1}$ to $0.0121\,kg\,m^{-2}$ at $50.0\,mm\,s^{-1}$. However, the difference in Fig. 13 drops from $0.0895\,kg\,m^{-2}$ at $24.2\,mm\,s^{-1}$ to $0.0228\,kg\,m^{-2}$ at $50.0\,mm\,s^{-1}$. Thus, at low casting speed, the flux consumption by the oscillation marks is similar for these two different practices. At high casting speed, however, the oscillation frequency increases in Fig. 13 in order to maintain constant pitch. This causes the oscillation mark consumption to roughly double, relative to the longer pitch for the fixed frequency of Fig. 17(b). More importantly, the lubrication consumption at high casting speed is higher for the constant or lower-frequency practice. This finding suggests that increasing the oscillation frequency with casting speed to maintain constant pitch may not be the best practice to optimize lubrication at high casting speed.

Figure 17(c) shows that introducing a non-sinusoidal oscillation mode, such as the 24% modification ratio investigated here, causes lubrication consumption to increase by ~10%. The total mold powder consumption also slightly increases, so this practice appears to be beneficial, as claimed in previous work,[8,43] although the effect is small.

8. Conclusions

A new model to predict mold powder consumption has been developed, based on measurements obtained under several different sets of controlled operation conditions during continuous casting of ultra-low carbon steel slabs. The model divides the total consumption into two components: the flux carried within the volume of the oscillation marks, and the remaining "lubrication consumption." The oscillation mark shape is based on plant measurements of oscillation mark depth, combined with the equilibrium meniscus shape from the balance between surface tension and gravity forces at the liquid steel/liquid slag interface, both before and after overflow. The estimated oscillation mark consumption is correlated with flux inflow during the negative strip time. This agrees with prior findings that oscillation marks in ultra-low carbon steel form *via* a meniscus freezing mechanism. A new equation to estimate oscillation mark depth is presented, which matches previous trends with oscillation stroke, frequency and negative strip time. The lubrication consumption is correlated with positive strip time. The two components of this new model suggest that accurate estimation of powder consumption should consider the effects of both negative and positive strip times. The effect of decreasing frequency and increasing modification ratio agrees with previous results, but no significant trend with stroke was predicted. Powder consumption infiltrated into the oscillation mark is the major component of slag consumption at slower casting speeds. Lubrication consumption is the major component at high speeds, where oscillation mark volume is small.

Acknowledgement

This work was supported by the Korea Research Foundation Grant (KRF-2003-013-D00150) for Seon-Hyo Kim.

Nomenclature

A_{OM}: Area of oscillation mark (mm^2)
D_{OM}: Depth of oscillation mark (mm)
d_{gap}: Mean distance between a solidifying shell and a mold wall (m)
f: Oscillation frequency (Hz)
g: Gravitational acceleration ($9.81\,m\,s^{-2}$)
k: Coefficient for oscillation mark depth de pending on mold powder (−)
N: Slab thickness (m)
$NSTR$: Negative strip time ratio (−)
P_{OM}: Pitch of oscillation marks (mm)
Q_{area}: Powder consumption per unit strand area ($kg\,m^{-2}$)
Q_{cons}: Weight of the bags consumed per one minute ($kg\,min^{-1}$)
Q_{OM}: Oscillation mark consumption per unit strand area ($kg\,m^{-2}$)
Q_{lub}: Lubrication consumption per unit strand area ($kg\,m^{-2}$)
q_{cycle}: Powder consumption per unit length in one cycle of oscillation ($g\,m^{-1}\,cycle^{-1}$)
q_{OM}: Oscillation mark consumption per unit length in one cycle of oscillation ($g\,m^{-1}cycle^{-1}$)
q_{lub}: Lubrication consumption per unit length in one cycle of oscillation ($g\,m^{-1}\,cycle^{-1}$)
s: Oscillation stroke (mm)

t_n: Negative strip time (s)
t_p: Positive strip time (s)
V_C: Casting speed ($m\,min^{-1}$)
v_s: Casting speed ($mm\,s^{-1}$)
W: Slab width (m)
W_{OM}: Width of oscillation mark (mm)
x: Distance perpendicular to the mold wall (m)
z: Distance along the mold wall (m)
α: Modification ratio for non-sinusoidal oscillation mode (%)
$\Delta\gamma$: Difference of surface tension between iquid steel and liquid slag ($N\,m^{-1}$)
ρ_{slag}: Density of liquid slag ($kg\,m^{-3}$)
$\Delta\rho$: Difference of density between liquid and liquid slag ($kg\,m^{-3}$)

REFERENCES

1) K. C. Mills and A. B. Fox: *ISIJ Int.*, **43** (2003), 1479.
2) F. B. Vieira: Steelmaking Conf. Proc., ISS-AIME, Warrendale, PA, (2002), 165.
3) M. M. Wolf: Steelmaking Conf. Proc., ISS-AIME, Warrendale, PA, (1991), 51.
4) C. A. M. Pinheiro, I. V. Samarasekera, J. K. Brimacombe, B. Howes and O. Gussias: *Ironmaking Steelmaking*, **27** (2000), 144.
5) J. Cho, H. Shibata, T. Emi and M. Suzuki: *ISIJ Int.*, **38** (1998), 440.
6) J. Konishi, M. Militzer, J. K. Brimacombe and I. V. Samarasekera: *Metall. Mater. Trans. B*, **33B** (2002), 413.
7) O. D. Kwon, J. Choi, I. R. Lee, J. W. Kim, K. H. Moon and Y. K. Shin: Steelmaking Conf. Proc., ISS-AIME, Warrendale, PA, (1991), 561.
8) M. Suzuki, H. Mizukami, T. Kitagawa, K. Kawakami, S. Uchida and M. Komatsu: *ISIJ Int.*, **31** (1991), 254.
9) S. Takeuchi, Y. Miki, S. Itoyama, K. Kobayashi, K. Sorimachi and T. Sakuraya: Steelmaking Conf. Proc., ISS-AIME, Warrendale, PA, (1991), 73.
10) M. Kawamoto, K. Nakajima, T. Kanazawa and K. Nakai: *ISIJ Int.*, **34** (1994), 593.
11) K. Tsutsumi, H. Murakami, S. Nishioka, M. Tada, M. Nakada and M. Komatsu: *Tetsu-to-Hagané*, **84** (1998), 617.
12) M. Suzuki, M. Suzuki, C. Yu and T. Emi: *ISIJ Int.*, **37** (1997), 375.
13) Y. Meng and B. G. Thomas: *Metall. Mater. Trans. B*, **34B** (2003), 685.
14) A. Yamauchi, K. Sorimachi, T. Sakuraya and T. Fujii: *ISIJ Int.*, **33** (1993), 140.
15) F. Neumann, J. Neal, M. A. Pedroza, A. H. Castillejos E. and F. A. Acosta G.: Steelmaking Conf. Proc., ISS-AIME, Warrendale, PA, (1996), 249.
16) C. Perrot, J. N. Pontoire, C. Marchionni, M. R. Ridolfi and L. F. Sancho: 5th European Continuous Casting Conf., L.R.d. Métallurgie, La Revue de Métallurgie, Nice, France, (2005), 36.
17) Y. Meng and B. G. Thomas: *Metall. Mater. Trans. B*, **34B** (2003), 707.
18) H. Nakato, T. Nozaki, Y. Habu, H. Oka, T. Ueda, Y. Kitano and T. Koshikawa: Steelmaking Conf. Proc., ISS-AIME, Warrendale, PA, (1985), 361.
19) S. Ogibayashi: Steelmaking Conf. Proc., ISS-AIME, Warrendale, PA, (2002), 175.
20) A. Yamauchi, T. Emi and S. Seetharaman: *ISIJ Int.*, **42** (2002), 1084.
21) B. G. Thomas, D. Lui and B. Ho: Effect of Transverse Depressions and Oscillation Marks on Heat Transfer in the Continuous Casting Mold, ed. by S. Viswanathan, R. G. Reddy and J. C. Malas, TMS, Warrendale, PA, (1997), 117.
22) J. J. Bikerman: Physical Surfaces, Academic Press, Inc., New York, (1970).
23) M. M. Wolf: Proc. 2nd European Conf. on Continuous Casting, VDEh, Düsseldorf, (1994), 78.
24) M. Suzuki, M. Suzuki and M. Nakada: *ISIJ Int.*, **41** (2001), 670.
25) S. Sridhar, K. C. Mills, O. D. C. Afrange, H. P. Lorz and R. Carli: *Ironmaking Steelmaking*, **27** (2000), 238.
26) M. M. Wolf: *Trans. Iron Steel Inst. Jpn.*, **20** (1980), 718.
27) H. Yasunaka, K. Nakayama, K. Ebina, T. Saito, M. Kimura and H. Matuda: *Tetsu-to-Hagané*, **81** (1995), 894.
28) T. Araki and M. Ikeda: *Can. Metall. Q.*, **38** (1999), 295.
29) T. Emi, H. Nakada, Y. Iida, K. Emoto, R. Tachibana, T. Imai and H. Bada: Steelmaking Conf. Proc., ISS-AIME, Warrendale, PA, (1978), 350.
30) P. Andrzejewski, A. Drastik, K. U. Kohler and W. Pluschkell: 9th PTD Conf. Proc., (1990), 173.
31) M. S. Jenkins: Heat Transfer in the Continuous Casting Mould, Ph. D Thesis, Monash University, Clayton, Vic., (1998).
32) M. Kawamoto, T. Murakami, M. Hanao, H. Kikuchi and T. Watanabe: Proc. of the Sixth Int. Conf. on Molten Slags, Fluxes and Salts, ed. by S. Seetharaman and D. Sichen, Division of Metallurgy, KTH, Sweden, Stockholm, Sweden–Helsinki, Finland, (2000), No. 146.
33) H. Nakato, S. Omiya, Y. Habu, T. Emi, K. Hamagami and T. Koshikawa: *JOM*, **36** (1984), 44.
34) M. Suzuki, S. Miyahara, T. Kitagawa, S. Uchida, T. Mori and K. Okimoto: *Tetsu-to-Hagané*, **78** (1992), 113.
35) S. Junghans: Process and Device for the Casting of Metal Strands, in German Patent 750 301, (1933).
36) E. Herrmann: Handbook of Continuous Casting, Aluminium-Verlag GmbH, Düsseldorf, (1958).
37) H.-P. Liu, S.-T. Qui, Y. Gan, H. Zhang and J.-Y. De: *Ironmaking Steelmaking*, **29** (2002), 180.
38) H.-J. Shin, G.-G. Lee, S.-M. Kang, S.-H. Kim, W.-Y. Choi, J.-H. Park and B. G. Thomas: *Iron Steel Technol.*, **2** (2005), 56.
39) H. Takeuchi, S. Matsumura, R. Hidaka, Y. Nagano and Y. Suzuki: *Tetsu-to-Hagané*, **69** (1983), 248.
40) A. W. Cramb and F. J. Mannion: Steelmaking Conf. Proc., ISS-AIME, Warrendale, PA, (1985), 349.
41) A. Howe and I. Stewart: Steelmaking Conf. Proc., ISS-AIME, Warrendale, PA, (1987), 417.
42) T. Okazaki, H. Tomono, K. Ozaki and H. Akahane: *Tetsu-to-Hagané*, **68** (1982), 265.
43) M. Inagaki, T. Hirose, C. Matsumura and J. Yamagami: *CAMP-ISIJ*, **2** (1989), 309.
44) K. Hamagami, K. Sorimachi and M. Kuga: Steelmaking Conf. Proc., ISS-AIME, Warrendale, PA, (1982), 358.
45) K. Kawakami, T. Kitagawa, H. Mizukami, S. Uchibori, S. Miyahara, M. Suzuki and Y. Shiratani: *Tetsu-to-Hagané*, **67** (1981), 1190.
46) Y. Itoh, S. Nabeshima and K. Sorimachi: Proc. of the Sixth Int. Conf. on Molten Slags, Fluxes and Salts, ed. by S. Seetharaman and D. Sichen, Division of Metallurgy, KTH, Sweden, Stockholm, Sweden–Helsinki, Finland, (2000), No. 152.
47) R. Bommaraju, T. Jackson, J. Lucas, G. Skoczylas and B. Clark: *Iron Steelmaker*, **19** (1992), 21.
48) J. M. Hill, Y. H. Wu and B. Wiwatanapataphee: *J. Eng. Math.*, **36** (1999), 311.
49) Y. Kobayashi and S. Maruhashi: 4th Japan-CSSR Seminar, CSSR, Ostrava, (1983).
50) I. Jimbo and A. W. Cramb: *Iron Steelmaker*, **20** (1994), 55.
51) R. Sato: Proc. National Open Hearth and Basic Oxygen Steel Conf., ISS AIME, Warrendale, PA, (1979), 48.
52) E. Takeuchi and J. K. Brimacombe: *Metall. Mater. Trans. B*, **15B** (1984), 493.
53) M. Olette: *Steel Res.*, **59** (1988), 246.
54) H. Gaye, L.-D. Lucas, M. Olette and P. V. Riboud: *Can. Metall. Q.*, **23** (1984), 179.
55) J. Lee and K. Morita: *ISIJ Int.*, **42** (2002), 599.
56) I. Jimbo and A. W. Cramb: *ISIJ Int.*, **32** (1992), 26.
57) J. Sengupta, H.-J. Shin, B. G. Thomas and S.-H. Kim: *Acta Mater.*, **54** (2006), 1165.
58) H. Yamamura, Y. Mizukami and K. Misawa: *ISIJ Int.*, **36** (1996), S223.
59) H. Tomono, W. Kurz and W. Heinemann: *Metall. Mater. Trans. B*, **12B** (1981), 409.
60) H.-J. Shin, B. G. Thomas, G.-G. Lee, J.-M. Park, C.-H. Lee and S.-H. Kim: MS&T 2004 Conf. Proc., The Association for Iron and Steel Technology (AIST) and TMS, Warrendale, PA, (2004), 11.
61) K. Tsutsumi, J. Ohtake and M. Hino: *ISIJ Int.*, **40** (2000), 601.
62) A. Badri, T. T. Natarajan, C. C. Snyder, K. D. Powers, F. J. Mannion, M. Byrne and A. W. Cramb: *Metall. Mater. Trans. B*, **36B** (2005), 373.
63) A. Badri, T. T. Natarajan, C. C. Snyder, K. D. Powers, F. J. Mannion and A. W. Cramb: *Metall. Mater. Trans. B*, **36B** (2005), 355.
64) J. Sengupta, B. G. Thomas, H.-J. Shin, G.-G. Lee and S.-H. Kim: *Metall. Mater. Trans. A*, **37A** (2006), 1597.
65) Y. Nakamori, Y. Fujikake, K. Tokiwa, T. Kataoka, S. Tsuneoka and H. Misumi: *Tetsu-to-Hagané*, **70** (1984), 1262.